Biorthogonal wavelets based Iris Recognition

Aditya Abhyankar[a], Lawrence Hornak[b] and Stephanie Schuckers[a,b]

[a] Department of Electrical and Computer Engineering,
Clarkson University, Potsdam, NY 13676, USA;
[b]Lane Department of Computer Science and Electrical Engineering
West Virginia University, Morgantown, West Virginia 26506, USA

ABSTRACT

Iris recognition has been demonstrated to be an efficient technology for doing personal identification. In this work, a method to perform iris recognition using biorthogonal wavelets is introduced. Effective use of biorthogonal wavelets using a lifting technique to encode the iris information is demonstrated. This new method minimizes built in noise of iris images using in-band thresholding in order to provide better mapping and encoding of the relevant information. Comparison of Gabor encoding, similar to the method used by Daugman and others, and biorthogonal wavelet encoding is performed. While Daugman's approach is a well-proven algorithm, the effectiveness of our algorithm is shown for the CASIA database, based on the ability to classify inter and intra class distributions, and may provide more flexibility for non-ideal images. The method was tested on the CASIA dataset of iris images with over 4,536 intra-class and 566,244 inter-class comparisons made. After calculating Hamming distances and for the selected threshold value of 0.4, FRR and FAR values were 13.6% and 0.6% using Gabor filter and 0% and 0.03% using the biorthogonal wavelets.

Keywords: iris recognition, biorthogonal wavelets, automatic segmentation, hamming distance, inter/intra class distribution, iris template, match scores

1. INTRODUCTION

Biometric identification is gaining more popularity and more acceptance in public as well as in private sectors. Iris recognition is considered to be highly accurate and reliable method of biometric identification. The iris, being found to be very stable, highly unique and easy to capture, is classified as one of the better biometric identifiers.[1, 2]

The unique epigenetic patterns of a human iris are used for personal identification. Image processing and signal processing techniques are employed to extract information from unique iris structure from a digitized image of an eye.[3–6] This information is encoded to formulate a "biometric template", which is stored in a database and also used for identification. Thus, the purpose of the template formation is to mathematically encode the iris pattern and match it with other similar representations. In this work, wavelet based iris recognition is developed and is compared with method similar to the well known Daugman's system.[3, 7–9] The designed system shows comparable results and is capable of further improvements to deal with non-ideal cases of iris recognition.

Following the general framework of Daugman's algorithm, the process of iris recognition is divided into four parts namely, *segmentation* where the iris region is isolated in an eye image under consideration; *mapping* where each pixel of the isolated iris is mapped from concentric domain to non-concentric domain; *encoding* where the filter coefficients are quantized and mapped into a binary bit stream giving rise to a template; and *matching* where 'Hamming distance' between every pair of the templates is calculated to find the inter and intra class distributions. The decision is made based on these distributions and various threshold values.

Wavelets are used for encoding the segmented iris information. To ensure efficiency of the system, a fast and efficient lifting scheme is used to design the biorthogonal wavelets.[10] Since a wavelet's basis has degrees

Further author information: (Send correspondence to Stephanie Schuckers)
Aditya Abhyankar: E-mail: abhyanas@clarkson.edu, Telephone:315-268-4404
Lawrence Hornak: E-mail: lah@csee.wvu.edu, Telephone:304-293-0405
Stephanie Schuckers: E-mail: sschucke@clarkson.edu, Telephone:315-268-6536

of freedom in two dimensions, their building blocks are very well localized in space as well as frequency. This property of wavelets is used to encode the iris information in an efficient way. Hamming distances are calculated from the encoded templates which essentially reflect the similarity score. The intra and inter class distributions are studied to determine whether the match is genuine or fake.[11, 12]

1.1. Data management

It is important to test the designed algorithm on sufficiently large and diverse data set. A data set of gray scale iris digital images provided by the Chinese Academy of Sciences (CASIA) is used for testing. The database consists of 756 gray scale images coming out of 108 distinct classes and 7 images of each eye. The data was collected from 80 subjects in two sessions with a one month gap between the two sessions.[13]

Also, the data was collected at 'eye center' at West Virginia University. This data was collected from 20 subjects in one session with 2 images of the left and right eye for each subject. Thus a total of 80 images coming from 40 classes are used for further testing of the algorithm. The CASIA data set predominantly has iris data from asians, while the data collected at the eye center mostly contains iris images of caucasians. Standard institutional review board procedures were utilized.

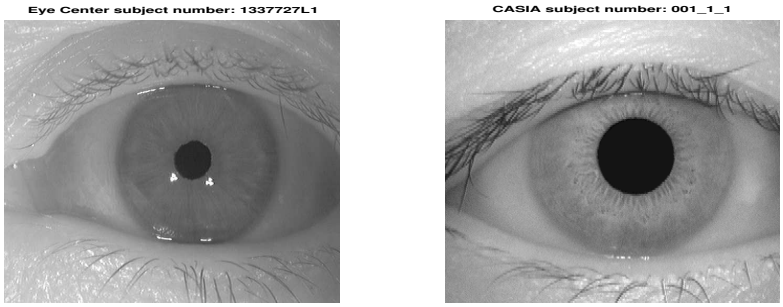

Figure 1. Sample iris images, where the left is a subject from WVU eye center and the right from CASIA.

Sample iris images are shown in Figure (1). It was concluded by inspecting visually that the iris images have sufficient resolution and clarity and hence no further enhancement techniques are used. The available data can be tabulated as follows:

Table 1. Data set: Distribution

Data set	No. of images	No. of classes	Exploited intra-class combinations	Exploited inter-class combinations
CASIA	756	108	4,536	566,244
Eye center	80	40	80	6320

1.2. Wavelet Analysis

For this particular study, the digital iris images are encoded using wavelets to formulate a template. Instead of traditional multiresolution analysis (MRA) scheme, a novel lifting technique is used to construct the biorthogonal filters.[10, 14–16] The main advantage of this scheme over the classical construction is that it does not rely on the Fourier transform. Also, it allows faster implementation of wavelet transform.

The basic idea behind the lifting scheme is shown in Figure (2). It starts with trivial wavelet, the "Lazy wavelet"; which has the formal properties of wavelet, but is not capable of doing the analysis. The lifting scheme then gradually builds a new wavelet, with improved properties, by adding in a new basis function. This itself is the inspiration behind the name of the scheme. The lifting scheme can be visualized as an extension of the FIR (Finite Impulse Response) schemes.[16]

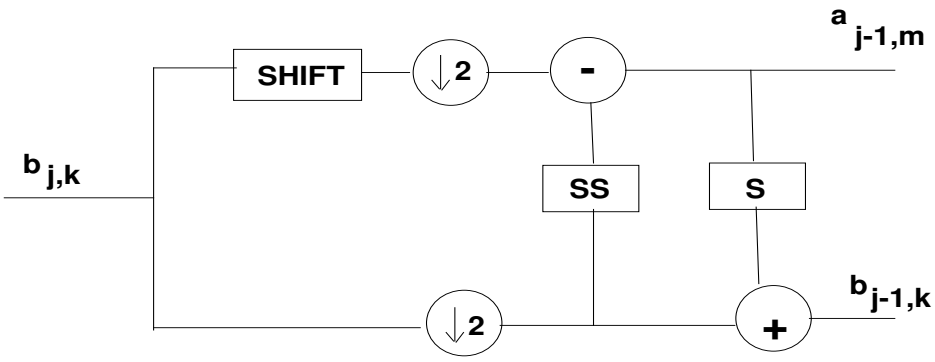

Figure 2. The lifting scheme for wavelets. It first calculates the Lazy wavelet transform, then calculates the $a_{j-1,m}$, and finally lifts the $b_{j-1,k}$.

It is known that any two-channel FIR sub band transform can be factored into a finite sequence of lifting steps. Thus, implementation of these lifting steps is faster and efficient. The biorthogonal filter family is shown in Figure (3). Biorthogonal 5/3 tap was selected for encoding the iris information. The frequency content of the resulting coefficients is adjusted each time to get separated band structure.

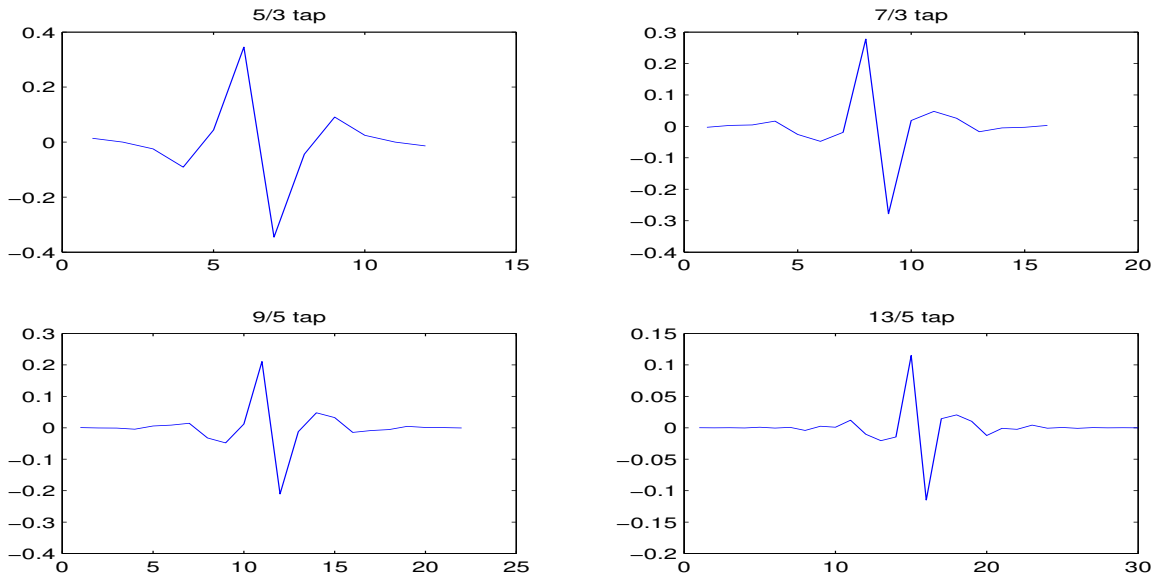

Figure 3. Biorthogonal filter family.

2. BI-ORTHOGONAL WAVELET BASED IRIS RECOGNITION

This section describes the algorithm developed to perform recognition for ideal conditions. The algorithm is flexible enough to be adapted for the non-ideal cases like off angle images, noise etc. The algorithm can be divided into following 4 steps:

1. Isolation or Segmentation
2. Normalization
3. Template Formation or Encoding

4. Match-Score Calculation

If we imagine a black box with all these functions incorporated, then the aim behind designing the system is to formulate an iris template after inputting the raw iris image. These functionalities are coded in MATLAB (v6.5R13) and a graphic user interface is developed. Although these steps are borrowed form Daugman's algorithm, the internal complexion of every step differs to Daugman's method, only in an attempt to make the system more efficient, either speed wise or performance wise.[17] The typical 'iris recognition system' is shown in Figure (4).

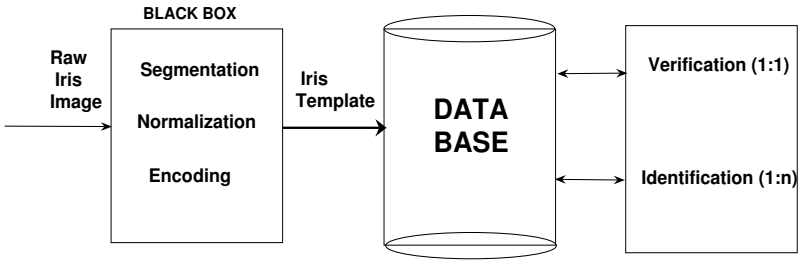

Figure 4. Typical Iris Recognition System.

2.1. Isolation or Segmentation

Segmentation involves isolating the important information from the rest of the eye image. Before doing actual segmentation, all the images are transformed into the wavelet domain and maxima energy extraction is performed. The number of retained coefficients is decided to be 10000. The images are inverse transformed before segmentation is performed using the log, simple gradient masking, and circular canny edge detection methodologies. The detected edges are mapped on the inverted iris images. The area within the global edge is phase shifted and then the complete image is transformed into the wavelet domain. The phase information is used and the marked area is further divided into smaller regions and average intensity thresholding is performed to further remove non-significant information. Non-significant information could be in the form of eye-lashes, eyelids and reflections.[18,19] In order to take care of these different types of noise entities, thresholding is done for each sub-band and hence the scheme is called 'in-band noise removal'. Each band significantly removes the noise content depending on whether it is high pass or low pass and the direction in which that filters acts i.e. horizontal, vertical or diagonal. E.g. eyelashes were predominantly removed in the HL band. The threshold value is adaptive and changes for every image depending upon the relative variations in the intensity of different parts of the image. The point where average intensity drops below the threshold is chosen as the iris radius. The threshold's effectiveness depends upon the angular resolution. However, increasing angular resolution may result in an excessively large template.

The circular resolution value of 20 is selected for this study, which is trade-off between providing effective division for noise removal as well as obtaining reasonable size templates. Sample isolated iris images are shown in Figure (5).

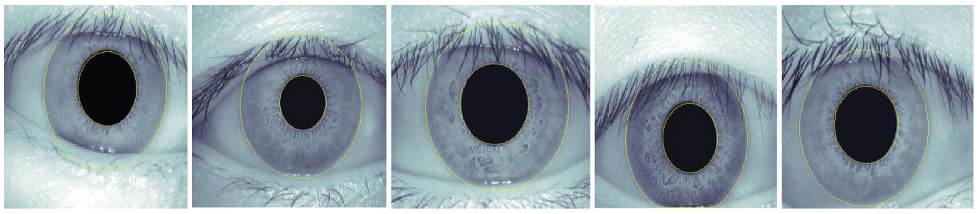

Figure 5. Sample isolated iris regions

2.2. Normalization

The first thing involved in the normalization process is to map the data from (r, θ) domain to (x, y) domain. For this the center of iris is taken as the starting point as against pupil center in the Daugman's method. The linear radial vector traces the complete iris region. Also, instead of matching up the iris and pupil centers, the vector dimension of the vector is kept fixed. This is the resolution along the iris radius. The vector dimension is fixed at 200. For highly non-concentric iris pupil pairs matching of the centers is performed. The diagonal information is mapped in the opposite quadrant to avoid any loss of information. An example of normalization is shown in Figure (6) with effects of more and less radial resolution shown clearly.

The reason behind high radial resolution of 200 against circular resolution of 20 can be explained as follows. After studying iris images using wavelets and examining their phase information, it was found that iris patterns have very strong components along the radial direction. This was concluded after observing average correlation among the wavelet coefficients along the radial direction to be 0.87 against average correlation of only 0.36 between wavelet coefficients of circular portions, on the normalized scale ranging from 0 to 1. The splitting was stopped when the energy of the correlated wavelet coefficients went below 20% of the total sub-band energy, and that number was retained as the resolution along circular or radial direction.

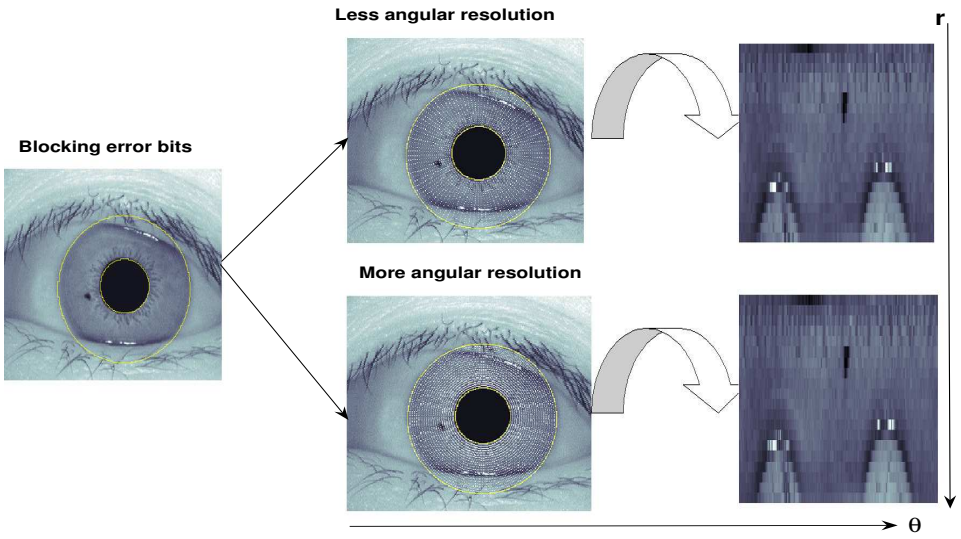

Figure 6. Process of iris normalization. Upper diagrams showing less angular resolution and lower part depicting more angular resolution.

2.3. Template Formation or Encoding

The segmented and normalized iris information is transformed into the wavelet domain using the biorthogonal tap, as explained earlier. The filters are designed using the lifting steps, which has the advantage that it is completely invertible. These filters transform the data into a different and new basis where 'large' coefficients correspond to relevant image data and 'small' coefficients corresponds to the noise. Thresholding is performed once again. The process is known as image de-noising. Wavelet encoded data is scalable and localized and hence matching of the features at same location using various scales is possible. A Gabor method is also implemented for comparison.[20] Band pass Gabor pre-filtering is performed to encode the information. The filter is generated using Gaussian filters and approximation is used. For both methods, the Gabor and wavelet coefficients are further quadrature quantized. This results in formation of bit-stream of $1s$ and $0s$. This is done for all the iris images and the formulated bit-pattern is called as 'iris template'. With angular resolution of 20 and radial resolution of 200, the formulated bit-streams are 8000 bits long. Along with the iris template, the mask template is also formed which is used for locating the noisy parts of the image.

2.4. Match score calculations

Only phase information converted to ones and zeros are encoded from the normalized iris patterns. The formulated templates are matched and similarity scores are calculated. Bit-wise comparison of the templates is made and Hamming distance is calculated for every such comparison. This is achieved by doing successive bit wise "X-OR"ing and "AND"ing. To account for the rotational inconsistencies the maximum matched value is chosen. The mask templates are used to ignore the noisy parts of the image. The formula for finding out the hamming distance is given in[7] as,

$$HD = \frac{\parallel (code\ A \otimes code\ B) \cap mask\ A \cap mask\ B \parallel}{\parallel mask\ A \cap mask\ B \parallel} \tag{1}$$

The operation of "X-OR" ($\otimes$) detects the dissimilarity between corresponding pair of bits, while "AND" ($\cap$) operation with the mask makes sure that the noisy or lesser significant portion of the image is not encoded. The ($\|\|$) represents the norm of the vectors. The Hamming Distances are normalized on the scale of a range from 0 to 1.

The whole algorithm in snap shot is given in Figure (7). (a) shows the original image while (b) shows the segmented iris image. The area between two marked circles is the significant iris information. The iris center is marked and used for normalization process. The effect of in-band de-noising for the selective iris area in shown in (c). For the selected value of radial resolution, iris area is divided along the radial direction and the distinct division is shown in (d). The normalized iris is shown in (e), while (f) shows the iris template. This particular sample iris is from CASIA data set.

3. RESULTS

753 out of 756 iris images were segmented accurately for CASIA data set and 77 out of 80 iris images were segmented accurately for eye-center data set. The images with inaccurately segmented iris region are not used for further analysis. The matching scores are divided into inter-class and intra-class matching. The distributions are graphed based on these calculated values. Inter-class results are the results obtained by matching iris of a person with iris of another person. Intra-class results are obtained by matching the template of a person with another template of the same iris, captured at other time. The distributions for both the classes are plotted and FAR (False Acceptance Rate) and FRR (False Rejection Rate) for different threshold values is calculated.

Table (2) gives the FRR and FAR values for information encoded using biorthogonal wavelets as well as Gabor filter. Match scores are calculated using hamming distance method. After calculating Hamming distances for the selected threshold values FRR and FAR values are given. A threshold of 0.4 results in FRR and FAR respectively ,of 13.6% and 0.6% using Gabor filter and 0% and 0.03% using the biorthogonal tap.

Figure (8) gives the results in detail. The hamming distance distributions are plotted for both type of filters for the entire data. To calculate the exact FRR and FAR values, the distributions of the hamming distances are calculated. The threshold value gives the classifier boundary. The intra class values above the boundary are treated as FRR values and the inter class below the boundary are treated as FAR values.

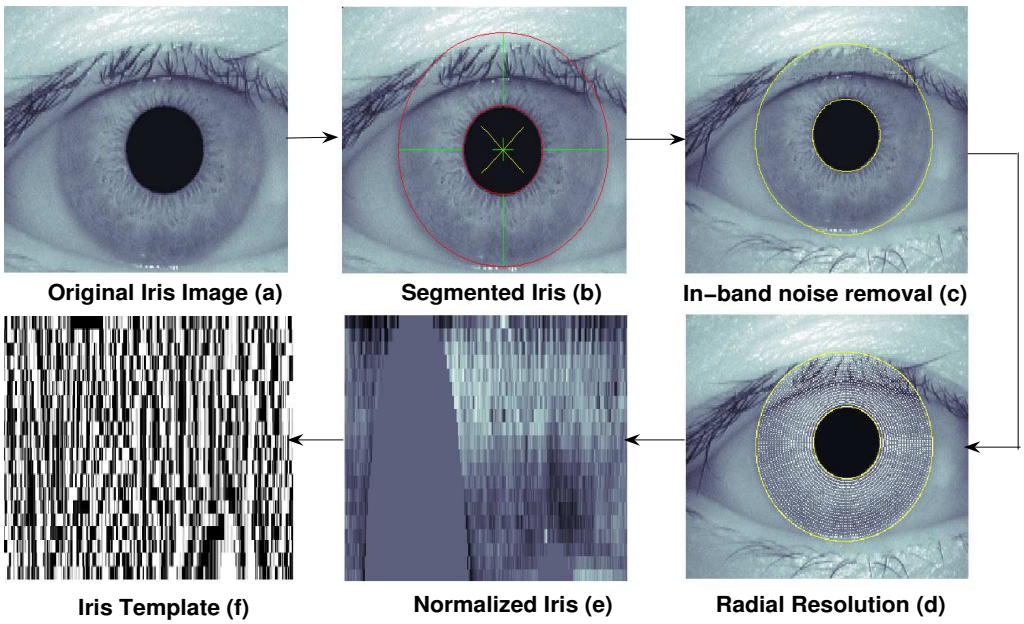

Figure 7. Complete algorithm in snap shot. The different stages are shown. segmentation, normalization and template formation.

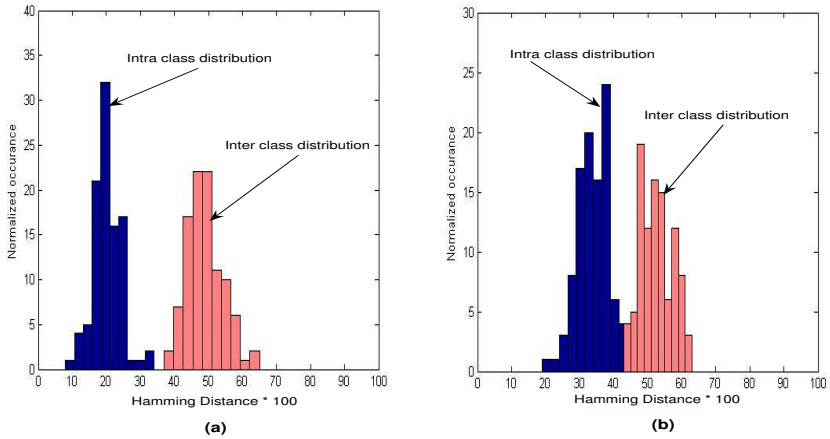

Figure 8. Results. (a) Inter and intra class Hamming distance distributions for biorthogonal filter and (b) Inter and intra class Hamming distance distributions for Gabor filter. *Normalized rate* is plotted on the y-axis, and *Hamming Distance*$*$ 100 is plotted on x-axis

Table 2. Results: FRR and FAR values for the selected threshold values and for selected filter type.

Biorthogonal wavelets			Gabor filters		
Threshold	FRR(%)	FAR(%)	Threshold	FRR(%)	FAR(%)
0.25	4.2	0.0	0.35	NA	NA
0.30	1.3	0.001	0.40	13.6	0.6
0.35	0.09	0.009	0.45	9.2	1.2
0.40	0.0	0.03	0.50	4.3	5.2
0.45	0.0	3.3	0.55	0.1	11.2

From the distributions and the FAR and FRR values it can easily seen that biorthogonal tap gives better results than Gabor filter. To model this mathematically, decidability index $d^{'}$ suggested by Daugman[7] is calculated to find out how well separated the inter and intra class distributions are. If μ_1 and μ_2 are the means and σ_{1b} and σ_{2b} the standard deviations of the distributions, then $d^{'}$ is calculated as,

$$d^{'} = \frac{|\mu_1 - \mu_2|}{\sqrt{(\sigma_1^2 + \sigma_2^2)/2}} \tag{2}$$

For biorthogonal tap $d^{'} = 7.5852$ and for Gabor filter $d^{'} = 2.8446$. The index value relies heavily on the filter parameters. The filter parameters can be fine tuned to further increase the separation between the two distributions and thus to improve the system accuracy.

4. CONCLUSION AND DISCUSSION

Biorthogonal wavelet based iris recognition system is designed and is shown to be capable of doing the personal identification with fairly high confidence. A good separation between inter and intra class Hamming distances is observed for biorthogonal case from figure (8). Although $d^{'}$ value is 7.5 against Daugman's 14.1[7] the dimensionality has also been reduced from 9600 to 8000. Unlike Daugman's fixed dimensionality, this dimensionality is adaptive and helps in finding the optimum dimension for the specific data set under consideration. Local maxima extraction is used to select the most significant image information, thus producing good segmentation results. The designed system is capable of doing the iris based personal identification.

ACKNOWLEDGMENTS

The work was funded by NSF IUCRC Center For Identification Technology Research (CITeR) and NSF grant ♯0325333.

REFERENCES

1. S.Noh, K.Pae, C.Lee, and J.Kim, "Multiresolution independent component analysis for iris identification," *The 2002 International Technical Conference on Circuits/Systems, Computers and Communications, Phuket, Thailand.* , 2002.
2. R. Wildes, "Iris recognition: an emerging biometric technology.," *Proceedings of the IEEE* **85**(9), 1997.
3. J. Daugman, "Biometric personal identification system based on iris analysis.," *United States Patent* **Patent Number: 5,291,560**, 1994.
4. W. Boles and B. Boashash, "A human identification technique using images of the iris and wavelet transform," *IEEE Transactions on Signal Processing* **46**(4), 1998.
5. L. Ma, Y. Wang, and T. Tan, "Iris recognition using circular symmetric filters. national laboratory of pattern recognition," *Institute of Automation, Chinese Academy of Sciences* , 2002.
6. R. Wildes, J. Asmuth, G. Green, S. Hsu, R. Kolczynski, J. Matey, and S. McBride, "A system for automated iris recognition," *Proceedings IEEE Workshop on Applications of Computer Vision, Sarasota, FL* , pp. 121–128, 1994.

7. J. Daugman, "How iris recognition works," *Proceedings of 2002 International Conference on Image Processing* **1**, 2002.
8. J. Daugman, "High confidence visual recognition of persons by a test of statistical independence.," *IEEE Transactions on Pattern Analysis and Machine Intelligence* **15**(11), 1993.
9. J. Daugman, "Biometric decision landscapes," *Technical Report No. TR482, University of Cambridge Computer Laboratory* , 2002.
10. W. Sweldens, "The lifting scheme: A new philosophy in biorthogonal wavelet constructions," in *Wavelet Applications in Signal and Image Processing III*, A. F. Laine and M. Unser, eds., pp. 68–79, Proc. SPIE 2569, 1995.
11. C. Tisse, L. Martin, L. Torres, and M. Robert, "Person identification technique using human iris recognition," *International Conference on Vision Interface* **Canada**, 2000.
12. Y. Zhu, T. Tan, and Y. Wang, "Biometric personal identification based on iris patterns," *Proceedings of the 15th International Conference on Pattern Recognition* **2**, 2000.
13. C. A. of Sciences Institute of Automation, "Database of 756 greyscale eye images," *http://www.sinobiometrics.com* , 2003.
14. I. Daubechies and W. Sweldens, "Factoring wavelet transforms into lifting steps," *J. Fourier Anal. Appl.* **4**(3), pp. 245–267, 1998.
15. R. Calderbank, I. Daubechies, W. Sweldens, and B.-L. Yeo, "Wavelet transforms that map integers to integers," *Appl. Comput. Harmon. Anal.* **5**(3), pp. 332–369, 1998.
16. W. Sweldens, "The lifting scheme: A construction of second generation wavelets," *SIAM J. Math. Anal.* **29**(2), pp. 511–546, 1997.
17. S. Lim, K. Lee, O. Byeon, and T. Kim, "Efficient iris recognition through improvement of feature vector and classifier," *ETRI Journal* **23**(2), 2001.
18. D. Z. W. Kong, "Accurate iris segmentation based on novel reflection and eyelash detection model," *Proceedings of 2001 International Symposium on Intelligent Multimedia, Video and Speech Processing* **Hong-Kong**, 2001.
19. N. Ritter, "Location of the pupil-iris border in slit-lamp images of the cornea," *Proceedings of the International Conference on Image Analysis and Processing* , 1999.
20. T. Lee, "Image representation using 2d gabor wavelets," *IEEE Transactions of Pattern Analysis and Machine Intelligence* **18**(10), 1996.